CELL CALCIUM

Cell Calcium (1995) **18**, 187–196

Calbindin-D_{28K} facilitates cytosolic calcium diffusion without interfering with calcium signaling

H.P.G. KOSTER, A. HARTOG, C.H. VAN OS and R.J.M. BINDELS

Department of Cell Physiology, University of Nijmegen, Nijmegen, The Netherlands

Abstract — The role of calbindin-D_{28K}, in transcellular Ca^{2+} transport and Ca^{2+} signaling in rabbit cortical collecting system was investigated. Rabbit kidney connecting tubules and cortical collecting ducts, hereafter referred to as cortical collecting system, were isolated by immunodissection and cultured to confluence on permeable filters and glass coverslips. Calbindin-D_{28K} was present in the cytosol of principal cells, but was absent from the intercalated cells. 1,25$(OH)_2D_3$ (48 h, 10^{-7} M) significantly increased cellular calbindin-D_{28K} levels (194 ± 15%) and stimulated transcellular Ca^{2+} transport (41 ± 3%). This stimulatory effect could be fully mimicked by the endogenous Ca^{2+} chelator, BAPTA (30 μM BAPTA/AM), which suggests that the presence of Ca^{2+} chelators alone is sufficient to enhance transcellular Ca^{2+} transport. Stimulation of Ca^{2+} transport was not accompanied by a rise in $[Ca^{2+}]_i$. Isosmotic replacement of extracellular Na^+ ($[Na^+]_o$) for N-methylglucamine (NMG) generated oscillations in $[Ca^{2+}]_i$ in individual cells of the monolayer. The functional parameters of these oscillations such as frequency of spiking, resting $[Ca^{2+}]_i$, increase in $[Ca^{2+}]_i$ and percentage of responding cells, were not affected by the level of calbindin-D_{28K}. In contrast, loading the cells with BAPTA abruptly stopped these $[Ca^{2+}]_i$ oscillations. This suggests that the kinetics of Ca^{2+} binding by calbindin-D_{28K} are slow relative to the initiation of the $[Ca^{2+}]_i$ rise, so that calbindin-D_{28K}, unlike BAPTA, is unable to reduce $[Ca^{2+}]_i$ rapidly enough to prevent the initiation of Ca^{2+}-induced Ca^{2+} release.

High affinity Ca^{2+}-binding proteins play a role in a large variety of cellular processes which are controlled by Ca^{2+}, including muscle contraction, neurotransmitter release, ion transport, and secretion [1,2]. This particular class of proteins shares a highly conserved Ca^{2+}-binding motif, the so-called EF-hand. One member of this family, i.e. calmodulin, is a ubiquitous protein, but the majority, like troponin-C, parvalbumin and calbindin, display a tissue-specific expression [1]. The physiological functions of some of these Ca^{2+}-binding proteins are firmly established, but for a few the expression 'more sites than insights' is appropriate [1]. For instance, calbindin-D_{28K} is present in high concentrations in distal nephron, placenta and brain [1–4]. In the epithelial tissues, calbindin-D_{28K} acts as a cytosolic Ca^{2+} buffer and presumably facilitates the diffusional flux of Ca^{2+} through the cytosol [5–7]. It is known that the rate of active Ca^{2+} absorption in the intestine correlates well with the cytosolic concentration of calbindin-D_{9K} and both phenomena are regulated by 1,25-dihydroxyvitamin D_3 (1,25$(OH)_2D_3$) [8,9]. In brain,

however, calbindin-D_{28K} is present in a subpopulation of neurons scattered in most but not all areas of the central nervous system, where its presence is not influenced by the vitamin D_3 status and where its function is unknown [1].

Free cytosolic Ca^{2+} ($[Ca^{2+}]_i$) is generally maintained at low resting values and, for example, increasing $[Ca^{2+}]_i$ in the intestine results in decreased NaCl absorption in villi and increased secretion in crypts [10]. Also, in renal cells, $[Ca^{2+}]_i$ is implicated in the regulation of transport processes. For example, Na^+ reabsorption and K^+ secretion in the distal nephron are partly regulated by activation of Ca^{2+}-dependent Na^+ and K^+ channels [11,12]. The cellular Ca^{2+} homeostasis in duodenum and distal nephrons is continuously challenged by large and variable rates of transcellular Ca^{2+} transport, which is tuned to the need of the body. In addition, calbindin-D_{28K} could, in theory, interfere with cellular Ca^{2+} signaling in view of its Ca^{2+} chelating properties.

In Ca^{2+} absorbing epithelial cells, the tuning of transcellular Ca^{2+} transport to cellular Ca^{2+} homeostasis is still poorly understood [13]. We have addressed this question by using a primary culture of renal connecting tubule and cortical collecting duct cells. These renal cells in culture retain the ability to transport Ca^{2+} transcellularly under control of PTH and $1,25(OH)_2D_3$ [14]. In addition, $[Ca^{2+}]_i$ oscillations can be provoked in these cells [15]. In the present study, the intracellular Ca^{2+} buffering capacity was manipulated by exposure to $1,25(OH)_2D_3$ to increase calbindin-D_{28K} content or by loading the cells with the Ca^{2+} ligand, BAPTA. Evidence is now provided that calbindin-D_{28K} enhances diffusional flux of Ca^{2+} but does not interfere with Ca^{2+} signaling. In contrast, BAPTA is shown to enhance transcellular Ca^{2+} transport, but quenches $[Ca^{2+}]_i$ oscillations completely.

Materials and methods

Isolation of rabbit kidney cortical collecting system cells

Rabbit kidney cortical collecting system cells were isolated from New Zealand white rabbits by immunodissection using monoclonal antibody R2G9 [14]. The cells were subsequently cultured in culture medium (equilibrated with 5% CO_2-95% air at 37°C) on circular glass coverslips (diameter = 22 mm) or on 0.3 cm^2 permeable filters (Costar, Badhoevedorp, The Netherlands) coated with rat tail collagen as described previously [14]. All experiments were performed on monolayers grown to confluency (4–7 days after seeding).

Fura–2 and BAPTA loading

Fura–2 was loaded into the cells during a 30 min incubation at 37°C in culture medium supplemented with 5 μM Fura–2 acetoxymethyl ester (Fura–2/AM), 0.4% (w/v) DMSO, 0.02% (w/v) Pluronic F127 and 4% (v/v) decomplemented fetal calf serum. Cells were loaded with the Ca^{2+} chelator BAPTA by exposure to incubation medium (at 37°C) containing 30 μM BAPTA/AM; 0.4% (w/v) DMSO; 0.02% (w/v) Pluronic F12 during the experiment.

Measurement of $[Ca^{2+}]_i$ in single cells

After loading the cells with Fura–2, the coverslips were transferred to a thermostated 'Leiden-Chamber' [15] and mounted on an inverted Diaphot microscope (Nikon, Amsterdam, The Netherlands). The cells were washed by superfusion with incubation medium for 3 min (2 ml/min, 37°C) after which, under continued superfusion, the experiment was started. The MagiCal imaging system was used to measure $[Ca^{2+}]_i$ (Joyce Loeble, UK). The Fura–2 loaded cells were alternatingly excited at 340 and 380 nm (bandwidth 10 nm) and images of the Fura–2 fluorescence of 30–40 cells emitted at 492 nm (bandwidth 30 nm) were captured (capture time 0.32 s; average of 8 frames) by a CCD camera at intervals of 7 s, using TARDIS software for digital analysis as described in detail by Neylon et al. [16]. In some experiments, the Newcastle Photometric System (NPS system) was used, in which Fura–2 fluorescence from single cells is measured by a photomultiplier as described previously [15]. $[Ca^{2+}]_i$ was calculated according to the formula derived by Grynkiewicz et al. [17].

Determination of transepithelial Ca^{2+} fluxes

Filter cups were washed and bathed at 37°C in incubation medium. Previously, we determined that transcellular Ca^{2+} absorption from a medium containing 1 mM Ca^{2+} was linear up to 3 h [18]. In the present study, Ca^{2+} absorption was established by removing duplicates of 25 µl apical fluid following an incubation of 90 min. The total Ca^{2+} concentration of the samples was assayed using a colorimetric test kit (Boehringer, Mannheim, Germany) and Ca^{2+} absorption was expressed in $nmol.h^{-1}.cm^{-2}$.

Identification of principal and intercalated cells by immunocytochemistry

The primary cultures contain principal and intercalated cells [15]. In order to distinguish intercalated cells [19], monolayers loaded with Fura–2, were exposed to FITC-conjugated peanut lectin (5 µg/ml for 5 min) and, before starting $[Ca^{2+}]_i$ measurements, the FITC-labelled monolayers were examined. Principal cells could be visualized after Fura–2 imaging by immunohistology using a polyclonal antiserum against chicken calbindin-D_{28K} as described previously [20]. As secondary antibody, an FITC-conjugated antirabbit Ig was used. One image of the resulting staining pattern was captured (excitation 490 nm, emission above 510 nm, MagiCal system) to match the presence of calbindin-D_{28K} or peanut lectin with $[Ca^{2+}]_i$ oscillations. Loading of principal cells with Fura–2 appeared to be far better than of intercalated cells and when the CCD camera was used $[Ca^{2+}]_i$ measurement in intercalated cells were unreliable. Therefore, in some experiments, a more sensitive photomultiplier (NPS system) was used to record fluorescence from Fura–2 loaded intercalated cells.

Calbindin-D_{28K} assay

An ELISA for calbindin-D_{28K} was performed as described previously [14]. Briefly a 96-well polystyrene plate was: (i) coated with 100 ng purified rabbit calbindin-D_{28K}; (ii) blocked with 0.1% w/v BSA: (iii) 50 µl samples containing either cytosolic fractions of cultured collecting system cells or samples of purified rabbit calbindin-D_{28K} for a calibration curve were added, both followed by 50 µl rabbit polyclonal antiserum against chick calbindin-D_{28K} (diluted 1:750); (iv) peroxidase-conjugated goat anti-rabbit IgG (H and L) (diluted 1:500) was added and finally 0.5 mg/ml *o*-phenylenediamine and 0.1 % w/v H_2O_2 were used to develop the color. After each step, the ELISA plate was washed 4 times.

Experimental procedures

Culture medium: DME/F12 (1:1) (Gibco, Breda, The Netherlands) supplemented with 5% (v/v) decomplemented fetal calf serum; 50 µg/ml gentamicin; 10 µ/ml non-essential amino acids (Gibco); 5 µg/ml insulin; 5 µg/ml transferrin; 50 nM hydrocortisone; 70 ng/ml PGE_1; 50 nM Na_2SeO_3; 5 pM triiodothyronine. Incubation medium (in mM): 140 NaCl; 2 KCl; 1 K_2HPO_4; 1 KH_2PO_4; 1 $MgCl_2$; 1 $CaCl_2$; 5 glucose; 5 L-alanine; 10 HEPES/Tris, pH 7.40. Fura–2/AM, BAPTA/AM and Pluronic F127 were obtained from Molecular Probes Inc. (Eugene, OR, USA). $1,25(OH)_2D_3$ was kindly provided by Solvay-Duphar (Weesp, The Netherlands). All other chemicals were obtained from Sigma (St Louis, MO, USA).

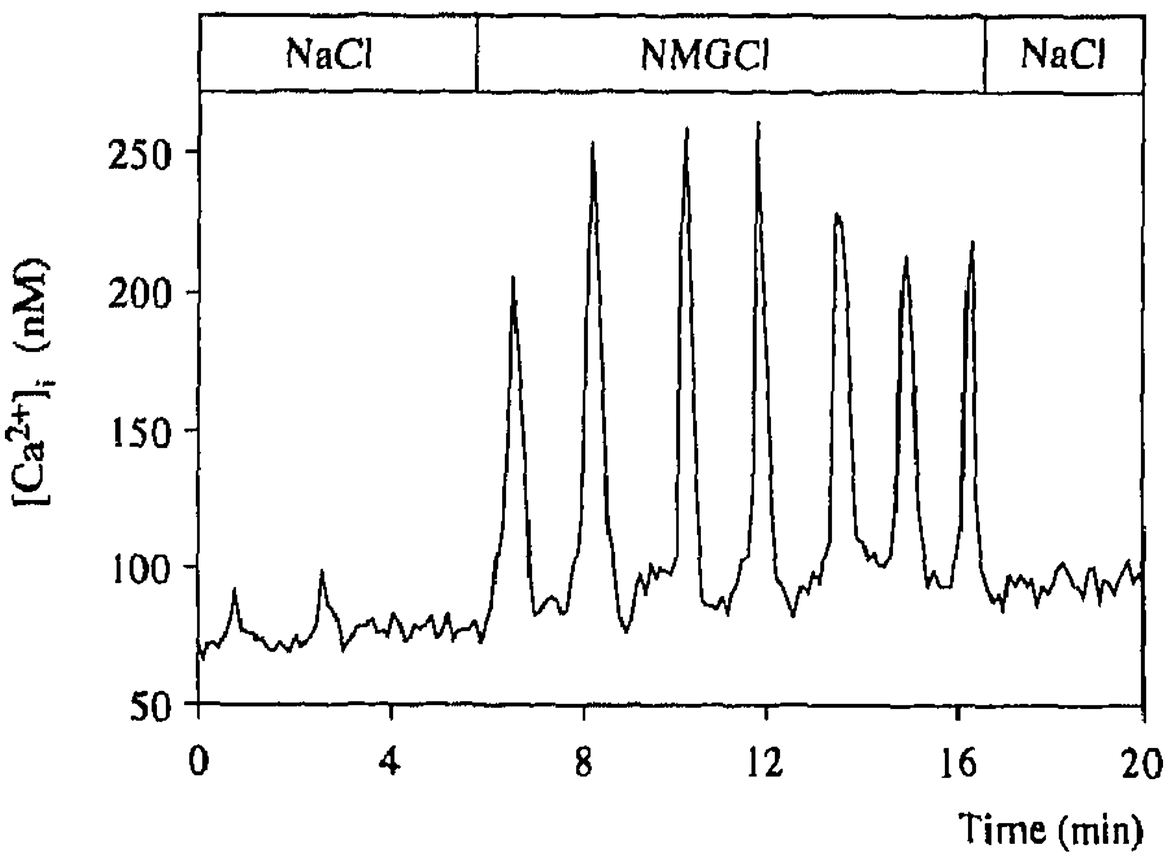

Fig. 1 Effect of removal of medium Na^+ (Na^+_o) on $[Ca^{2+}]_i$ in cultured cells from rabbit cortical collecting system. Na^+_o (NaCl) was iso-osmotically replaced with N-methylglucamine (NMGCl). $[Ca^{2+}]_i$ was calculated from the Fura–2 340/380 nm excitation fluorescence emission ratio which was recorded with the fluorescence imaging MagiCal system. Representative trace from 6 experiments is shown, in which a total of 36 cells were analyzed.

Statistical analysis

In all experiments, data were assessed from at least 3 isolations. Analysis of variance was used to determine statistical differences between two independent groups [21].

Results

In a previous study, we described that in cells of cortical collecting system in primary culture, removal of extracellular Na^+ induced oscillations of $[Ca^{2+}]_i$, which arise from phospholipase C activation in concert with Ca^{2+}-induced Ca^{2+} release [15]. The present study extends our previous observations by employing a fluorescence imaging system equipped with a CCD camera which permits simultaneous analysis of the $[Ca^{2+}]_i$ responses of several cells at the single cell level and estimation of cytosolic calbindin-D_{28K} content. Isosmotic replacement of medium Na^+ (Na^+_o) for N-methylglucamine (NMG) results in $[Ca^{2+}]_i$ oscillations in primary cultures of rabbit cortical collecting system cell. The type of oscillations most frequently observed (~80% of the occurrences) was an increase in $[Ca^{2+}]_i$ in an oscillatory fashion with Ca^{2+} returning to resting levels in between two spikes, as shown in Figure 1.

Characterization of $[Ca^{2+}]_i$ oscillations in principal and intercalated cells

Since the primary culture of rabbit cortical collecting system is composed of two cell types, individual

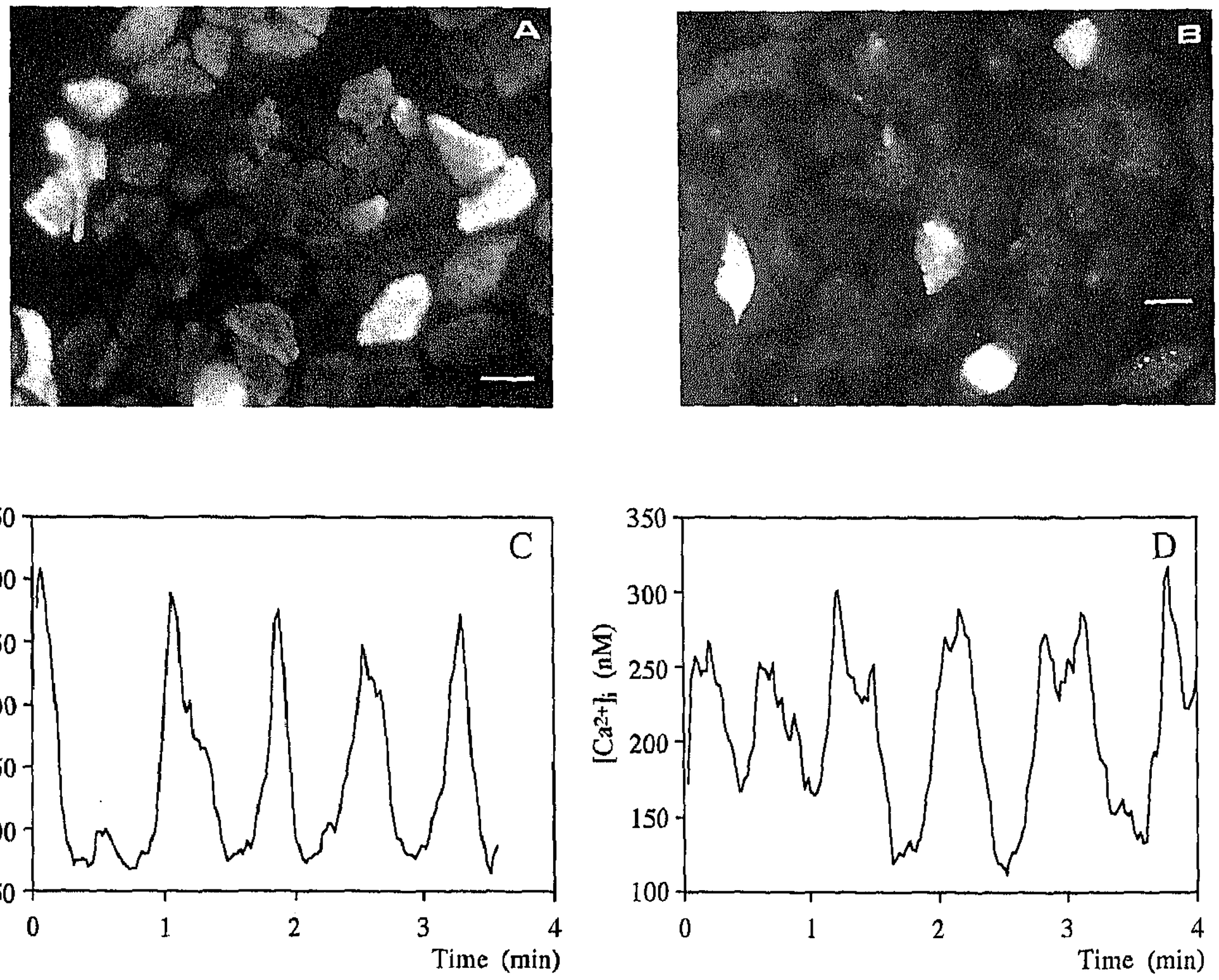

Fig. 2 Na^+_o-free induced $[Ca^{2+}]_i$ oscillations in a principal (**A,C**) and an intercalated (**B,D**) cell of rabbit cortical collecting system in primary culture. $[Ca^{2+}]_i$ was calculated from the Fura–2 340/380 nm excitation fluorescence emission ratio which was recorded with the NPS system. Monolayers were double stained to distinguish principal from intercalated cells. Principal cells were recognized by immunohistological staining with a polyclonal antibody against chicken calbindin-D_{28K} (**A**) and intercalated cells were identified by exposure to FITC-conjugated peanut lectin (**B**). Bars represent 10 μm. Representative data from 6 experiments are shown, in which a total of 36 cells were analyzed.

Table 1 Characterisation of Na^+_o-free induced $[Ca^{2+}]_i$ oscillations in principal and intercalated cells recorded with the NPS system. Resting and peak $[Ca^{2+}]_i$, oscillations frequency and percentage of cells showing oscillations when exposed to Na^+ free medium. Values represent mean ± SE with n ≥ 19.

Cell type	*Resting $[Ca^{2+}]_i$ (nM)*	*Peak $[Ca^{2+}]_i$ (nM)*	*Frequency (min^{-1})*	*Oscillating cells (%)*
Intercalated cells	116 ± 11	261 ± 30	0.59 ± 0.05	73 ± 8
Principal cells	123 ± 14	326 ± 28	0.64 ± 0.06	65 ± 13

cells were identified by immunocytochemistry, using peanut lectin to recognize intercalated cells and an antiserum against chicken calbindin-D_{28K} to recognize principal cells (Fig. 2A,B) [19]. The majority of cells (79 ± 4%, n = 400) were calbindin-D_{28K} positive and peanut lectin negative and, therefore, identified as principal cells, whereas a minority (18 ± 5%) were calbindin-D_{28K} negative and peanut lectin positive and classified as intercalated cells. In principal cells, calbindin-D_{28K} was evenly distributed throughout the cytosol.

Na^+_o-free medium induced in both cell types oscillatory increases in $[Ca^{2+}]_i$ as depicted in Figure 2. The characteristics of these oscillations, i.e. oscillatory frequency, resting and peak values of $[Ca^{2+}]_i$, together with the percentage of cells that exhibit $[Ca^{2+}]_i$ oscillations, are shown in Table 1. There were no significant differences between these parameters among principal and intercalated cells ($P < 0.05$, ≥ 19).

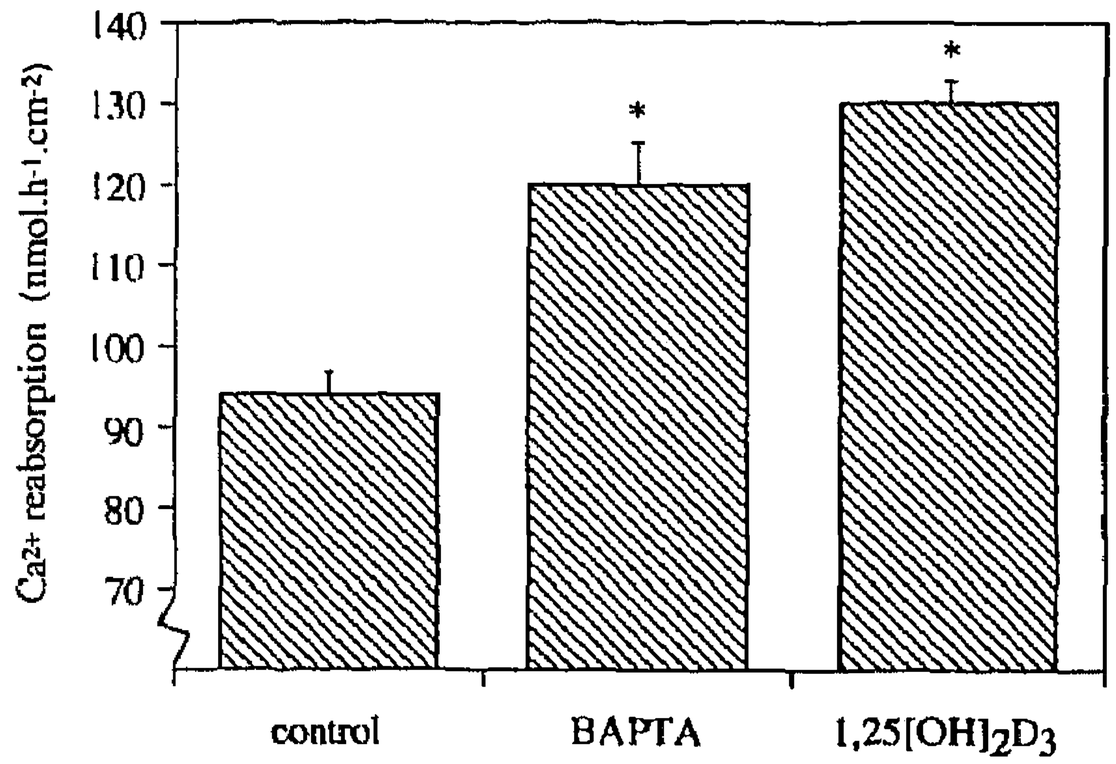

Fig. 3 Effect of the Ca^{2+} chelator BAPTA and $1,25(OH)_2D_3$ on active transcellular Ca^{2+} transport across rabbit cortical collecting system in primary culture. Monolayers were exposed to BAPTA/AM (3×10^{-5} M for 2 h), 1,25(OH)2D3 (10^{-7} M for 48 h) or vehicle (control) as indicated. Values are means ± SE of 4 experiments; *significantly different from control ($P < 0.05$).

Effect of $1,25(OH)_2D_3$ on Ca^{2+} transport, calbindin-D_{28K} content and Ca^{2+} signaling

The monolayers were incubated for 48 h with 10^{-7} M $1,25(OH)_2D_3$ and subsequently transcellular Ca^{2+} transport, cellular calbindin-D_{28K} content and $[Ca^{2+}]_i$ oscillations were examined. $1,25\{OH]_2D_3$ $1,25(OH)_2D_3$ when compared with control cells significantly increased transcellular Ca^{2+} transport by 41 ± 3% (Fig. 3) and calbindin-D_{28K} content from 0.69 ± 0.09 to 2.03 ± 0.31 μg.mg protein^{-1} ($P > 0.2$, n = 4). However, the characteristics of $[Ca^{2+}]_i$ oscillations were not significantly altered in principal cells cultured for 2 days in the presence of

Table 2 Characterisation of Na^+_o-free induced $[Ca^{2+}]_i$ oscillations in principal cells exposed to 10^{-7} M $1.25(OH)_2D_3$ for 48 h (or to vehicle) measured with the fluorescence imaging MagiCal system. Resting and peak $[Ca^{2+}]_i$, oscillations frequency and percentage of cells showing oscillations when exposed to Na^+ free medium. Values represent mean ± SE with n ≥ 100.

Condition	*Resting $[Ca^{2+}]_i$ (nM)*	*Peak $[Ca^{2+}]_i$ (nM)*	*Frequency (min^{-1})*	*Oscillating cells (%)*
Control	98 ± 6	201 ± 4	0.71 ± 0.02	79 ± 8
$1,25(OH)_2D_3$	108 ± 6	214 ± 4	0.73 ± 0.02	66 ± 6

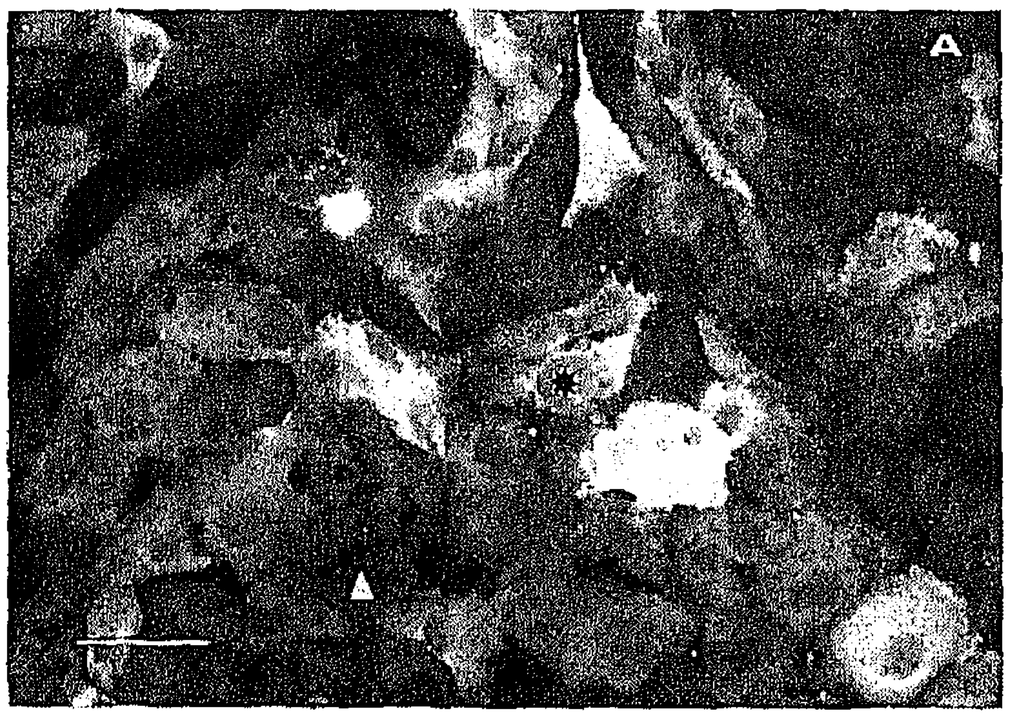

Fig. 4 Effect of calbindin-D_{28K} concentration on Na^+_o-free induced $[Ca^{2+}]_i$ oscillations in principal cells of rabbit cortical collecting system in primary culture. Principal cells were recognized by immunohistological staining with a polyclonal antibody against chicken calbindin-D_{28K} (A). $[Ca^{2+}]_i$ oscillations were analyzed in a cell with a relatively low (cell Δ, B) and a relatively high (cell *, C) level of calbindin-D_{28K}, respectively. $[Ca^{2+}]_i$ was calculated from the Fura–2 340/380 nm excitation fluorescence emission ratio which was recorded with the fluorescence imaging MagiCal system. Bar represents 20 μm. Representative data from 4 experiments are shown, in which a total of 32 cells were analyzed.

(Table 2).

To corroborate further the interaction between calbindin-D_{28K} and Ca^{2+} signaling, we compared within one single monolayer characteristics of $[Ca^{2+}]_i$ oscillations in principal cells expressing different levels of calbindin-D_{28K}. In line with the above mentioned results, principal cells containing different concentrations of calbindin-D_{28K} exhibit identical $[Ca^{2+}]_i$ oscillations (Fig. 4, n = 32).

Effect of BAPTA on Ca^{2+} transport and Ca^{2+} signaling

Loading cells of the cortical collecting system with the Ca^{2+} chelator BAPTA (30 μM BAPTA/AM) significantly ($P < 0.05$, n = 4) enhanced transcellular Ca^{2+} transport by 28 ± 5% (Fig. 3). Resting $[Ca^{2+}]_i$, however, was not influenced by BAPTA. $[Ca^{2+}]_i$ was 108 ± 3 and 98 ± 3, ($P > 0.2$, n = 24) for control and BAPTA-loaded cells, respectively (Fig. 5A). On the contrary, when proximal tubule cells in primary culture, which lack calbindin-D_{28K}, are loaded with BAPTA, $[Ca^{2+}]_i$ is lowered from

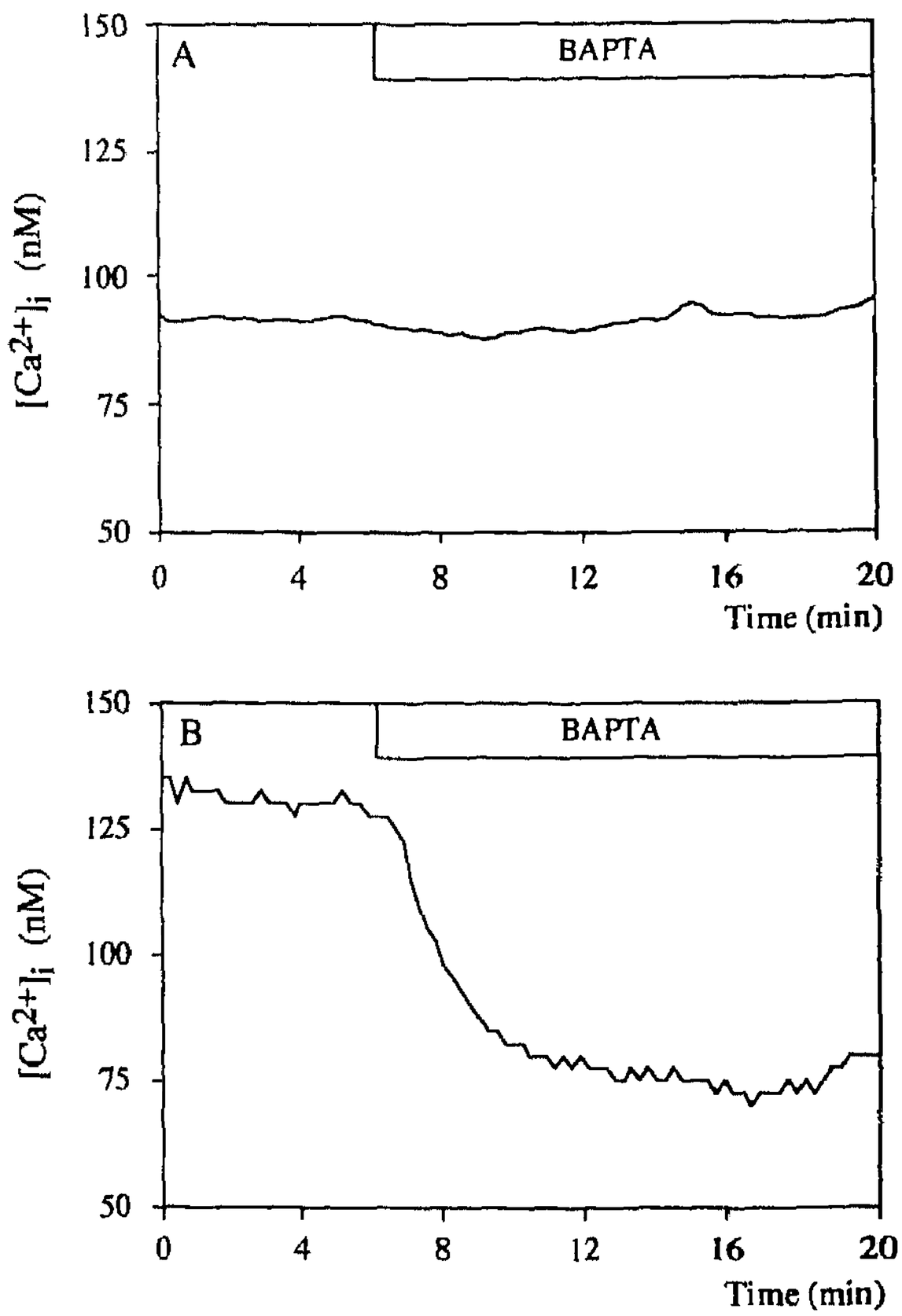

Fig. 5 Effect of the Ca^{2+} chelator BAPTA on resting $[Ca^{2+}]_i$ in principal cells of rabbit cortical collecting system in primary culture (A) and in cells of rabbit proximal tubules in primary culture (B). Monolayers were incubated in BAPTA/AM (3×10^{-5} M). $[Ca^{2+}]_i$ was calculated from the Fura–2 340/380 nm excitation fluorescence emission ratio which was recorded with the fluorescence imaging MagiCal system. Representative traces from 4 experiments are shown, in which a total of 24 cells were analyzed.

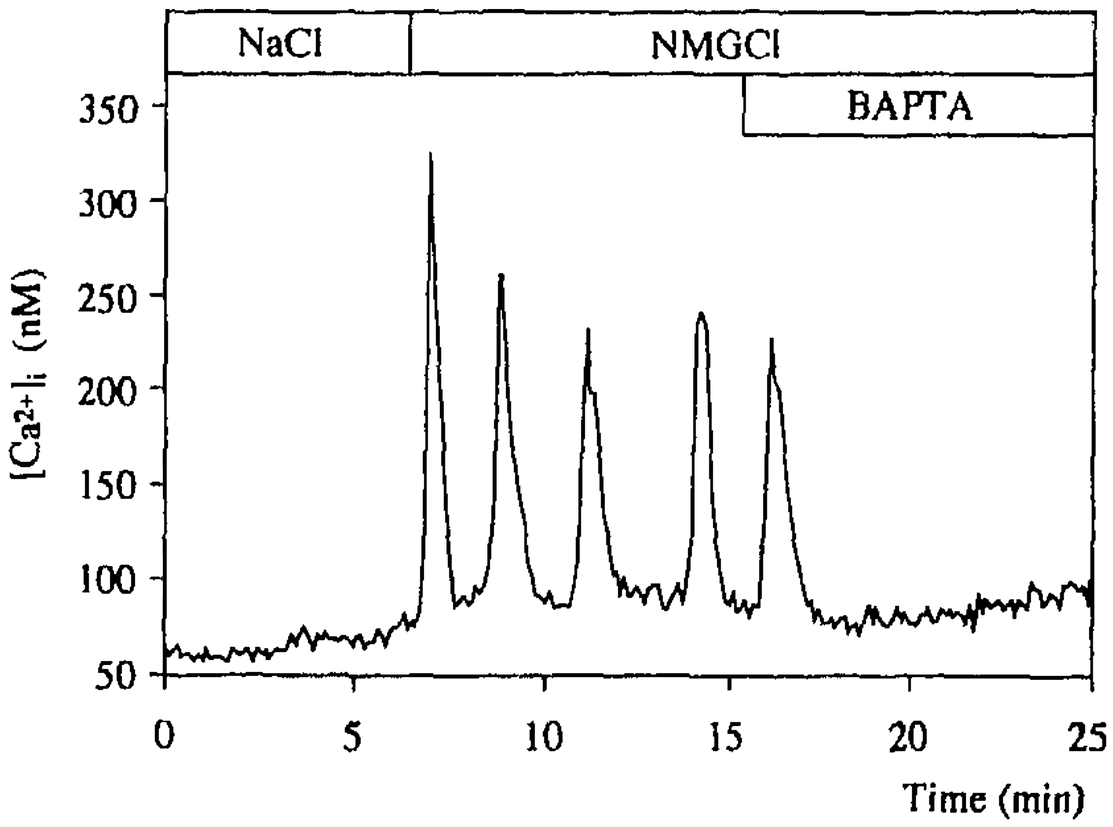

Fig. 6 Effect of the Ca^{2+} chelator BAPTA on Na^+_o-free induced $[Ca^{2+}]_i$ oscillations in principal cells of rabbit cortical collecting system in primary culture. Na^+_o (NaCl) was isoosmotically replaced with N-methylglucamine (NMGCl) and monolayers were subsequently incubated in BAPTA/AM (3×10^{-5} M). $[Ca^{2+}]_i$ was calculated from the Fura–2 340/380 nm excitation fluorescence emission ratio which was recorded with the fluorescence imaging MagiCal system. A representative trace from 4 experiments is shown, in which a total of 24 cells were analyzed.

169 ± 2 to 86 ± 3, ($P < 0.05$, n = 24) (Fig. 5B). In striking contrast to calbindin-D_{28K}, addition of BAPTA/AM (30 μM) to the incubation medium interrupted $[Ca^{2+}]_i$ oscillations within 1.9 ± 0.2 min (Fig. 6, n = 24).

Discussion

The present study demonstrates that increased levels of cytosolic Ca^{2+} ligands, as calbindin-D_{28K} and BAPTA, stimulate active transcellular Ca^{2+} transport in the rabbit cortical collecting system. In addition, calbindin-D_{28K} does not interfere with $[Ca^{2+}]_i$ signaling, while BAPTA completely inhibits $[Ca^{2+}]_i$ oscillations.

Feher et al. developed a mathematical model which explains the role of calbindin-D_{9K} in $1,25(OH)_2D_3$-stimulated intestinal Ca^{2+} absorption [6,8]. In this model, calbindin enhances transcellular Ca^{2+} transport by: (i) stimulating apical entry of Ca^{2+} through releasing the negative feedback on the entrance step; (ii) increasing the rate of cytosolic transport by acting as a diffusional carrier; (iii) increasing Ca^{2+} efflux rate by feeding Ca^{2+} to the starved basolateral Ca^{2+}-ATPase and Na^+/Ca^{2+} exchanger. The present study provides experimental evidence for a stimulatory effect of Ca^{2+} ligands on transcellular Ca^{2+} transport in the cortical collecting system. We localized calbindin-D_{28K} in the cytosol of principal cells, where concentrations reach 100 μM [14]. An increase in calbindin-D_{28K} content was accompanied by an increase in the rate of transcellular Ca^{2+} transport. This stimulatory effect of calbindin-D_{28K} could be fully mimicked by the Ca^{2+} chelator, BAPTA, which strongly suggests that the presence of diffusible Ca^{2+} chelators alone is sufficient to enhance transcellular Ca^{2+} transport. This implies that Ca^{2+} chelators influence Ca^{2+} fluxes at the entrance and exit step [6]. An increased Ca^{2+} buffer capacity in close vicinity to the apical membrane could accelerate the entry of Ca^{2+}, due to removing a negative-feedback of $[Ca^{2+}]_i$ on the influx mechanism. Ca^{2+} efflux could be enhanced by Ca^{2+} ligands by accelerated delivery of Ca^{2+} to the basolateral extrusion pumps [6].

In the present study, stimulated rates of transcellular Ca^{2+} transport were not accompanied by an increase in $[Ca^{2+}]_i$. Furthermore, addition of BAPTA did not reduce resting $[Ca^{2+}]_i$ in principal cells of the cortical collecting system, whereas in cells which lack calbindin-D_{28K}, BAPTA substantially reduced $[Ca^{2+}]_i$. These findings support the notion that calbindin-D_{28K} greatly enhances the intrinsic Ca^{2+} buffering capacity of principal cells.

The role of calbindin-D_{28K} as a strong Ca^{2+}

Table 3 Chelator forward and reverse rate constants for the Ca^{2+} chelator/Ca^{2+} binding (k_{on} and k_{off}), and dissociation constants are given for BAPTA and calbindin-D_{28K}.

Chelator	k_{on} $(M^{-1} \cdot s^{-1})$	k_{off} (s^{-1})	K_d *(nM)*	*Reference*
BAPTA	6.02×10^8	96.7	100–500	[23]
Calbindin-D_{28K}	2×10^7	8.6	430	[6]

buffer seems in conflict with the fact that $[Ca^{2+}]_i$ fluctuations are an essential step in regulatory pathways, since an increased Ca^{2+} buffering capacity most likely dampens the transient rise in $[Ca^{2+}]_i$ evoked by receptor activation. The present study, however, clearly demonstrates that calbindin-D_{28K} does not interfere with Ca^{2+} signaling processes, since oscillations in $[Ca^{2+}]_i$ could be provoked irrespective of the absence or presence of calbindin-D_{28K} in the cell. In contrast, loading the cells with BAPTA abruptly stopped the $[Ca^{2+}]_i$ oscillations. This remarkable difference between both calcium chelators must reside in the Ca^{2+} binding kinetics. The difference is not explained on the basis of Ca^{2+} affinities, since the K_ds of both Ca^{2+} ligands for Ca^{2+} are similar (*see* Table 3). It is theoretically possible that BAPTA reaches significantly higher cytosolic concentrations than calbindin-D_{28K}. When hypocampal neurons were incubated for 30 min at 37°C with 30 μM BAPTA/AM the intracellular BAPTA concentration reached ~300 μM [22]. We observed that within 2 min after addition of 30 μM BAPTA/AM, the $[Ca^{2+}]_i$ oscillations stopped, which implies that the cytosolic concentration of BAPTA does not differ widely from the cytosolic calbindin-D_{28K} concentration, which was estimated to be ~100 μM [14]. The most plausible explanation for the observed differences is that the k_{on} rate of Ca^{2+} binding to calbindin-D_{28K} is too slow, so that calbindin-D_{28K}, unlike BAPTA, is unable to reduce the upstroke of a Ca^{2+} spike rapidly enough to prevent the initiation of Ca^{2+}-induced Ca^{2+} release. The k_{on} rate is in fact more than one order of magnitude slower for calbindin-D_{28K} than for BAPTA (Table 3). Indeed, calbindin has been reported to buffer Ca^{2+} sluggishly when compared to troponin and calmodulin [4]. A similar explanation accounted for differences between EGTA and BAPTA in attenuating Ca^{2+}-activated K^+ currents in chromaffin cells and in reducing evoked neurotransmitter release at the squid giant synapse [23].

Until now, little is known about the role of calbindin-D_{28K} in non-epithelial cells, such as Purkinje cells in the cerebellum, specific neurons in the brain and several endocrine cells [1–4]. The characteristics of calbindin-D_{28K} outlined in the present study should also hold in these tissues. For example, calbindin-D_{28K} will bind Ca^{2+} in the cytosol during intense neural activity and thus protects neurons from Ca^{2+} overload. After these Ca^{2+} pulses, calbindin-D_{28K} will facilitate redistribution of Ca^{2+} within the cell which could mediate stimulation-evoked changes in neuronal cell shape or mediate memory effects in brain [4,24,25]. Roberts made a theoretical analysis of a mechanism by which millimolar concentrations of calbindin-D_{28K} found in certain sensory receptors and neurons can influence $[Ca^{2+}]_i$ signaling [26]. He demonstrated that high levels of calbindin-D_{28K} are necessary to serve as a mobile Ca^{2+} buffer that reduces and localizes changes in $[Ca^{2+}]_i$ by shuttling Ca^{2+} away from the Ca^{2+} channel arrays. Indeed, in rat sensory neurons, it has been shown that injection of high concentrations of calbindin-D_{28K} into the cell has no effect on basal $[Ca^{2+}]_i$, but affects the kinetics of $[Ca^{2+}]_i$ increase [27]. Our findings in epithelial cells

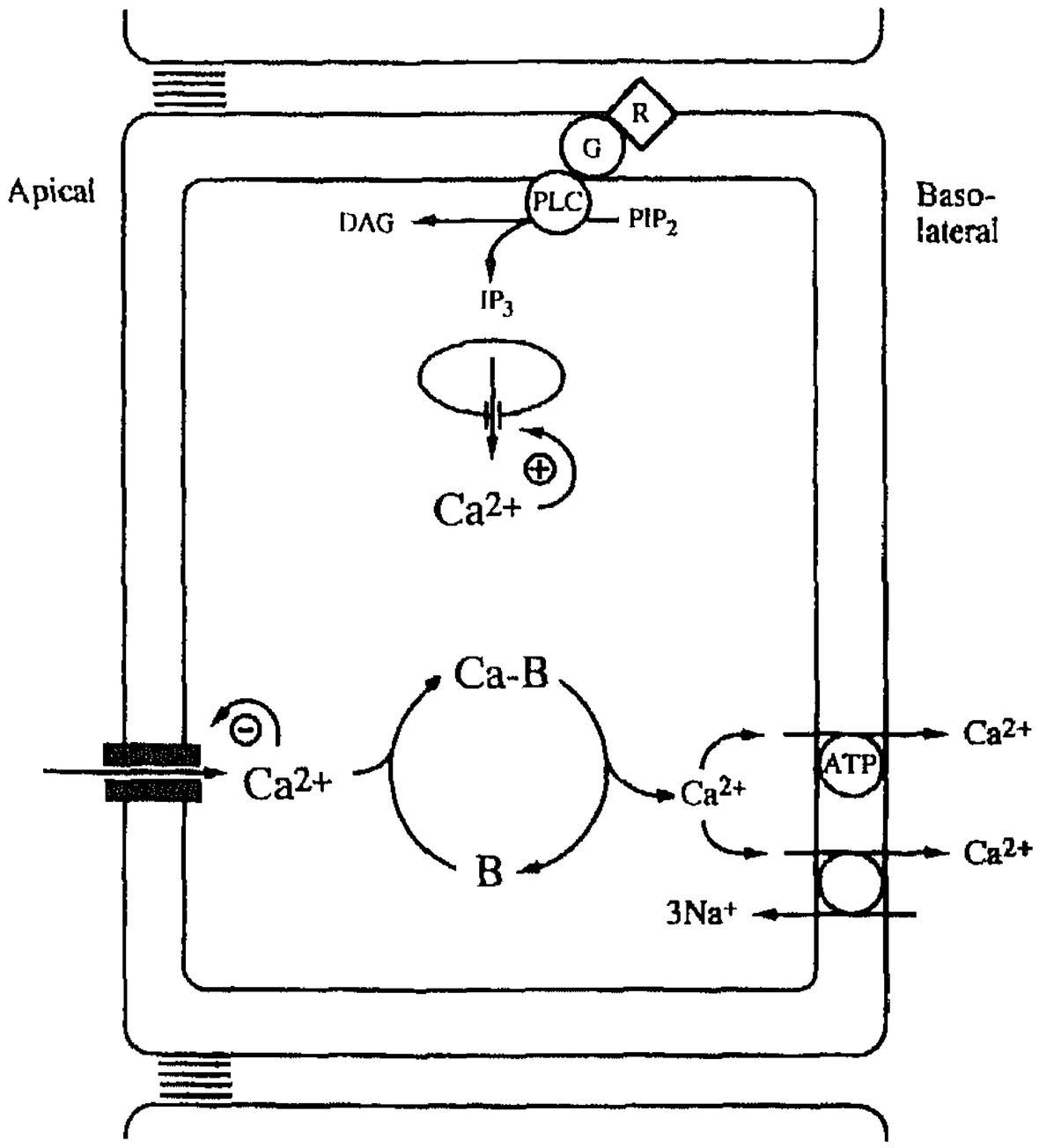

Fig. 7 Model of transcellular Ca^{2+} transport and Ca^{2+} signaling processes co-operating in principal cells of the cortical collecting system. For an explanation see text. B, a calcium ligand such as calbindin-D_{28K} or BAPTA; DAG, diacylglycerol; IP_3, inositol 1,4,5-trisphosphate; PIP_2, phosphatidylinositol 4,5-bisphosphate; G, G-protein; PLC, phospholipase C; R, receptor.

show that with lower, i.e. submillimolar, levels of calbindin-D_{28K}, there is no interference with Ca^{2+} signaling. Also, in a previous study by Muir et al. [28], a similar conclusion was reached. These investigators stably expressed calbindin-D_{28K} in NIH3T3 cells and the presence of calbindin-D_{28K} did not affect resting $[Ca^{2+}]_i$ nor did it change the increase in $[Ca^{2+}]_i$ which occurred in response to serum stimulation.

The findings of the present study can be summarized in a model shown in Figure 7. Transcellular Ca^{2+} movement involves the sequential transport of Ca^{2+} across the apical membrane, cytosol and basolateral membrane. The apical entry mechanism is still unidentified, but is postulated to be inhibited by high $[Ca^{2+}]_i$ adjacent to the apical membrane, referred to as a negative-feedback inhibition of Ca^{2+} entry [6]. Calbindin-D_{28K} binds Ca^{2+} ions which enter the cytosol and facilitates cytosolic diffusion. Finally, calbindin-D_{28K} increases the supply of Ca^{2+} to the Ca^{2+} pumps in the basolateral membrane [6]. During transcellular Ca^{2+} movement, $[Ca^{2+}]_i$ remains constant. Due to the slow binding kinetics of calbindin-D_{28K}, Ca^{2+} signaling can occur independently of transcellular Ca^{2+} movement mediated by calbindin-D_{28K}. The summarized properties of calbindins are compatible with substantial cytosolic Ca^{2+} diffusion and protection of the cell from being flooded with Ca^{2+} and guarantees an unaltered $[Ca^{2+}]_i$ signaling in epithelial cells involved in transcellular Ca^{2+} transport.

Acknowledgements

The authors thank Dr H. Raat for determining the effect of BAPTA on $[Ca^{2+}]_i$ of proximal tubules in primary culture. Mrs A. Hartog was supported by a grant from the Dutch Kidney Foundation (#91.1112).

References

1. Heizmann CW. Hunziker W. (1991) Intracellular calcium-binding proteins: more sites than insights. TIBS, 16, 98-103.
2. Heizmann CW. (1992) Calcium-binding proteins: basic concepts and clinical implications. Gen. Physiol. Biophys., 11, 411-425.
3. Williams RJP. (1992) Calcium fluxes in cells – new views on their significance. Cell Calcium, 13, 273-275.
4. Williams RJP. (1994) Calcium-binding proteins in normal and transformed cells. Cell Calcium, 16, 339-346.
5. Gross M. Kumar R. (1990) Physiology and biochemistry of vitamin D-dependent calcium binding proteins. Am. J. Physiol., 259, F195-F209.
6. Feher JJ. Fullmer CS. Wasserman RH. (1992) Role of facilitated diffusion of calcium by calbindin in intestinal calcium absorption. Am. J. Physiol., 262, C517-C526.
7. Bindels RJM. (1993) Calcium handling by the mammalian kidney. Exp. Biol., 184, 89-104.
8. Feher JJ. (1983) Facilitated calcium diffusion by intestinal calcium-binding protein. Am. J. Physiol., 244, C303-C307.
9. Bronner F. Pansu D. Stein WD. (1986) An analysis of intestinal calcium transport across the rat intestine. Am. J. Physiol., 250, G561-G569.
10. Homaidan FR. Donowitz M. Weiland GA. Sharp GWP. (1989) Two calcium channels in basolateral membranes of rabbit ileal epithelial cells. Am. J. Physiol., 257, G86-G93.
11. Hébert RL. Jacobson HL. Breyer MD. (1991) Prostaglandin E_2 inhibits sodium transport in rabbit cortical collecting duct by increasing intracellular calcium. J. Clin. Invest., 87, 1992-1998.
12. Schlatter E. Bleich M. Hirsch J. Markstahler U. Frobe U. Greger R. (1993) Cation specificity and pharmacological properties of the Ca^{2+}-dependent K^+ channel of rat cortical collecting ducts. Pflügers Arch., 422, 481-491.
13. Bourdeau JE. Lau K. (1992) Regulation of cytosolic free calcium concentration in the rabbit connecting tubule. A calcium-absorbing renal epithelium. J. Lab. Clin. Med., 119, 650-662.
14. Bindels RJM. Hartog A. Timmermans J. van Os CH. (1991) Active Ca^{2+} transport in primary cultures of rabbit kidney CCD. Stimulation by 1,25-dihydroxyvitamin D_3 and PTH. Am. J. Physiol., 261, F799-F807.
15. Koster HPG. Van Os CH. Bindels RJM. (1993) Ca^{2+} oscillations in the rabbit renal cortical collecting system induced by Na^+ free solutions. Kidney Int., 43, 828-836.
16. Neylon CB. Hoyland J. Mason WT. Irvine RF. (1990) Spatial dynamics of intracellular calcium in agonist-stimulated vascular smooth muscle cells. Am. J. Physiol., 259, C675-C686.
17. Grynkiewicz G. Poenie M. Tsien RY. (1985) A new generation of Ca^{2+} indicators with greatly improved fluorescence properties. J. Biol. Chem., 260, 3440-3450.
18. Bindels RJM. Hartog A. Abrahamse SL. van Os CH. (1994) Effects of pH on apical calcium entry and active calcium transport in rabbit cortical collecting system. Am. J. Physiol., 266, F620-F624.
19. Schuster VL. Bonsib SM. Jennings ML. (1986) Two types of collecting duct mitochondria-rich (intercalated) cells. Lectin and band 3 cytochemistry. Am. J. Physiol., 251, C347-C355.
20. Bindels RJM. Timmermans JAH. Hartog A. Coers W. van Os CH. (1991) Calbindin-D_{9k} and parvalbumin are exclusively located along basolateral membranes in rat distal nephron. J. Am. Soc. Nephrol., 2, 1122-1129.
21. Snedecor GW. Cochran WG. (1974) Statistical methods. Ames, Iowa: The Iowa State University Press.

22. Fredholm BB, Hu PS. (1993) Effect of an intracellular calcium chelator on the regulation of electrically evoked [^{3}H]-noradrenaline release from rat hippocampal slices. Br. J. Pharmacol., 108, 126-131.
23. Adler EM, Augustine GJ, Duffy SN, Charlton MP. (1991) Alien intracellular calcium chelators attenuate neurotransmitter releases at the squid giant synapse. J. Neurosci., 11, 1496-1507.
24. Rogers J. (1989) The search for functions. Nature, 339, 661-662.
25. Kasai H. (1993) Cytosolic Ca^{2+} gradients, Ca^{2+} binding proteins and synaptic plasticity. Neurosci. Res., 16, 1-7.
26. Roberts WM. (1994) Localization of calcium signals by a mobile calcium buffer in frog saccular hair cells. J. Neurosci., 14, 3246-3262.
27. Chard PS, Bleakman D, Christakos S, Fullmer CS, Miller RJ. (1993) Calcium buffering properties of calbindin-D_{28K} and parvalbumin in rat sensory neurones. J. Physiol., 472, 341-357.
28. Muir EM, Lawson DEM, Sepúlveda FV, O'Brien JA, Harding M. (1993) Calbindin-D_{28K} expression in transfected mouse NIH3T3 cells. Cell Calcium, 14, 349-358.

Please send reprint requests to : Dr René J.M. Bindels, 162 Cell Physiology, University of Nijmegen, PO Box 9101, 6500 HB Nijmegen, The Netherlands.

Received : 9 March 1995
Accepted : 9 June 1995